Molecular Cell
Article

The Nuclear Poly(A)-Binding Protein Interacts with the Exosome to Promote Synthesis of Noncoding Small Nucleolar RNAs

Jean-François Lemay,[1] Annie D'Amours,[1] Caroline Lemieux,[1] Daniel H. Lackner,[2] Valérie G. St-Sauveur,[1] Jürg Bähler,[2] and François Bachand[1,*]
[1]RNA Group, Department of Biochemistry, Université de Sherbrooke, Sherbrooke, QC JIH 5N4, Canada
[2]Department of Genetics, Evolution and Environment and UCL Cancer Institute, University College London, London WC1E 6BT, UK
*Correspondence: f.bachand@usherbrooke.ca
DOI 10.1016/j.molcel.2009.12.019

SUMMARY

Poly(A)-binding proteins (PABPs) are important to eukaryotic gene expression. In the nucleus, the PABP PABPN1 is thought to function in polyadenylation of pre-mRNAs. Deletion of fission yeast *pab2*, the homolog of mammalian *PABPN1*, results in transcripts with markedly longer poly(A) tails, but the nature of the hyperadenylated transcripts and the mechanism that leads to RNA hyperadenylation remain unclear. Here we report that Pab2 functions in the synthesis of noncoding RNAs, contrary to the notion that PABPs function exclusively on protein-coding mRNAs. Accordingly, the absence of Pab2 leads to the accumulation of polyadenylated small nucleolar RNAs (snoRNAs). Our findings suggest that Pab2 promotes poly(A) tail trimming from pre-snoRNAs by recruiting the nuclear exosome. This work unveils a function for the nuclear PABP in snoRNA synthesis and provides insights into exosome recruitment to polyadenylated RNAs.

INTRODUCTION

Polyadenylation of RNA is fundamental to posttranscriptional gene regulation. In eukaryotes, the 3′ poly(A) tail is generally thought to confer positive roles in the mRNA life cycle, such as nuclear export competence, stability, and translational activity. In contrast to these positive roles, recent studies in humans, plants, and yeast reveal that the poly(A) tail can also target an RNA for degradation via the nuclear exosome (Chekanova et al., 2007; LaCava et al., 2005; Vanacova et al., 2005; Wang et al., 2008; West et al., 2006; Wyers et al., 2005).

The exosome complex is one of the primary systems that operates in RNA processing and degradation in eukaryotes. Although the exosome is evolutionarily conserved, it has been most extensively studied in *Saccharomyces cerevisiae*. In this organism, the exosome is composed of nine catalytically inactive polypeptides to which is associated the active 3′→5′ exonuclease, Rrp44/Dis3 (Houseley et al., 2006; Ibrahim et al., 2008; Lebreton and Seraphin, 2008; Schmid and Jensen, 2008; Vanacova and Stefl, 2007). Because inactivation of the exosome via depletion or mutation of any of these ten subunits perturbs similar steps in RNA processing, they are often referred to as the core exosome. The core exosome is found in the nucleus and the cytoplasm. In the nucleus, the activity of the core exosome is associated with an additional 3′→5′ exonuclease, Rrp6 (Allmang et al., 1999b). Despite the physical association between Rrp6 and the nuclear exosome, genetic and biochemical evidence indicates that they can perform distinct roles in RNA processing (Allmang et al., 1999a; Callahan and Butler, 2008; Grzechnik and Kufel, 2008; Milligan et al., 2005; Mitchell et al., 2003; van Hoof et al., 2000).

Polyadenylation-dependent exosome processing can lead to the complete digestion or the partial 3′ end trimming of a substrate RNA (Houseley et al., 2006; Lebreton and Seraphin, 2008; Schmid and Jensen, 2008; Vanacova and Stefl, 2007). As yet, the molecular details behind the choice between 3′ end maturation and complete degradation by the exosome are not clearly understood. Poly(A)-dependent exosome activation is promoted by a polyadenylation complex called TRAMP (for Trf4/5-Air1/2-Mtr4 polyadenylation complex). Notably, the polymerase activity of the TRAMP complex is not mediated by the canonical nuclear poly(A) polymerase (Pap1 in *S. cerevisiae*) that catalyzes mRNA polyadenylation but via the product of the *TRF4* or *TRF5* genes in *S. cerevisiae* (Houseley and Tollervey, 2006; Vanacova et al., 2005; Wyers et al., 2005) and the *cid14* gene in *S. pombe* (Win et al., 2006). Although TRAMP-mediated polyadenylation is believed to mark most RNAs that are destined for exosome-dependent processing, the accumulation of specific polyadenylated transcripts in *RRP6Δ* cells reduces after inactivation of Pap1 (Carneiro et al., 2007; Grzechnik and Kufel, 2008; van Hoof et al., 2000), suggesting a role for the canonical poly(A) polymerase in exosome-dependent processing.

The importance of exosome-dependent gene regulation is highlighted by the many different types of nuclear RNAs that are targeted by this pathway, including aberrant pre-mRNAs (Bousquet-Antonelli et al., 2000; Milligan et al., 2005; Saguez et al., 2008; West et al., 2006), unprocessed rRNAs (Allmang et al., 1999a, 2000; Dez et al., 2006), unmodified tRNAs (Kadaba et al., 2006; Vanacova et al., 2005), cryptic unstable transcripts (Arigo et al., 2006; Vasiljeva et al., 2008; Wyers et al., 2005), and small nuclear (sn) and small nucleolar (sno)

RNAs (Allmang et al., 1999a; Grzechnik and Kufel, 2008; van Hoof et al., 2000). snoRNAs are an important class of nonpolyadenylated RNAs that assemble into ribonucleoprotein (RNP) particles to act in pre-rRNA processing and modification (Reichow et al., 2007). snoRNAs can be divided into two functional classes depending on the type of pre-rRNA modification that is promoted: box C/D snoRNAs guide 2′-O-ribose methylation, whereas box H/ACA snoRNAs guide pseudouridylation. While the majority of yeast snoRNAs are independently transcribed as larger precursors by RNA polymerase II, a limited number are encoded from intronic sequences of pre-mRNAs (Kiss et al., 2006). A polyadenylation-independent maturation pathway that involves 3′→5′ trimming of 3′-extended precursors by the exosome has been proposed for the synthesis of independently transcribed yeast snoRNAs (Carroll et al., 2004; Fatica et al., 2000; Kim et al., 2006; Steinmetz et al., 2001; Vasiljeva and Buratowski, 2006). However, a recent study suggests that a polyadenylation step is important for pre-snoRNA 3′ end processing via the nuclear exosome (Grzechnik and Kufel, 2008). Yet the mechanism by which 3′ poly(A) tails recruit the nuclear exosome to specific transcripts remains poorly understood.

The evolutionarily conserved nuclear poly(A)-binding protein (PABP2/PABPN1) is the nuclear counterpart of the well-studied cytosolic PABP (PABPC1 in humans and Pab1 in yeast). PABPN1 is characterized by a putative coiled-coil region, a single RNA recognition motif, and a carboxy-terminal glycine/arginine-rich domain (Kuhn and Wahle, 2004; Mangus et al., 2003). Experiments using in vitro assays suggest that PABPN1 plays essential roles in mRNA polyadenylation: (1) PABPN1 stimulates processive poly(A) synthesis by direct and simultaneous interactions with the poly(A) polymerase and the growing poly(A) tail (Kerwitz et al., 2003); and (2) PABPN1 promotes, via a poorly defined mechanism, the transition from processive to distributive synthesis after addition of ~200–300 adenine residues (Wahle, 1995). We have recently reported the identification of a PABPN1 homolog in the fission yeast *Schizosaccharomyces pombe* (Perreault et al., 2007). Notably, deletion of *S. pombe pab2* results in the expression of RNAs with hyperadenylated tails (Perreault et al., 2007); yet the mechanism that leads to hyperadenylation remains unknown.

Here we used DNA microarrays to identify hyperadenylated transcripts detected in *pab2Δ* cells. Using this genome-wide approach, we found that the absence of Pab2 leads to the accumulation of polyadenylated snoRNAs, and we describe the molecular mechanism of their accumulation. We find that Pab2 is recruited to the 3′ end of snoRNA-encoding genes, is bound to polyadenylated snoRNAs, and is physically associated with the nuclear exosome, suggesting that Pab2 recruits the exosome to promote 3′ end processing of polyadenylated pre-snoRNAs. Our results have therefore unveiled an example of a PABP involved in the synthesis of noncoding RNAs.

RESULTS

Small Nucleolar RNAs Are Upregulated in *pab2Δ* Cells

We previously reported that *pab2Δ* cells display hyperadenylated RNAs (Perreault et al., 2007). In principle, poly(A) tail extension could influence RNA metabolism and modulate gene expression. Accordingly, a genome-wide strategy was established to investigate for gene expression changes in *pab2Δ* cells to distinguish between a general or a specific effect of Pab2 on RNA polyadenylation. Reverse transcription steps prior to microarray analysis were randomly primed to prevent any bias due to poly(A) tail length differences between wild-type and *pab2Δ* cells. A global comparison between wild-type and *pab2Δ* cells is presented in Figure 1A. Notably, the expression levels of most genes were unaffected by the deletion of *pab2*. A statistical analysis was used (Tusher et al., 2001) to identify RNAs that significantly changed their expression levels between wild-type

A

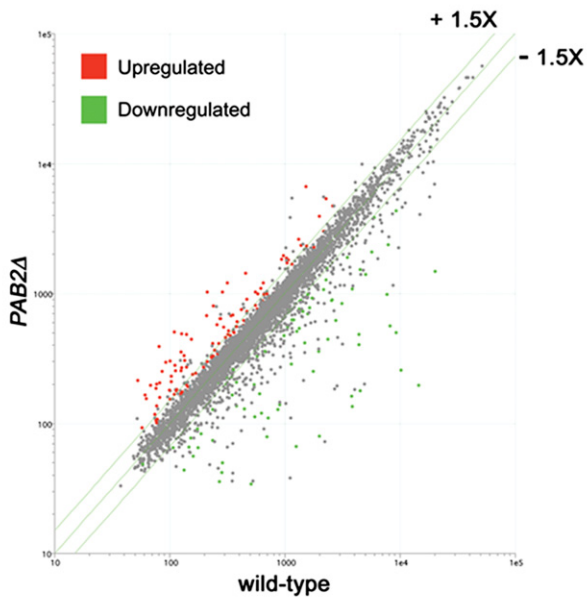

B

Systematic ID		Common Name	Average Ratio	Type
SPSNORNA.51	*	*SNR99*	4.90	H/ACA
SPSNORNA.52		*SNR101*	2.53	H/ACA
SPSNORNA.47		*SNR95*	2.38	H/ACA
SPSNORNA.37	*	*SNR10*	2.23	H/ACA
SPSNORNA.35		*SNR3*	2.17	H/ACA
SPSNORNA.40	*	*SNR42*	2.12	H/ACA
SPSNORNA.50		*SNR98*	1.91	H/ACA
SPSNORNA.46	*	*SNR94*	1.87	H/ACA
SPSNORNA.20		*SNOU17*	1.53	H/ACA
SPSNORNA.34		*SNO20/SNR35*	1.26	H/ACA
SPSNORNA.25		*SNOZ30*	1.25	C/D

Figure 1. Gene-Specific Changes in Expression Level in the *pab2Δ* Strain

(A) Scatter plot of the RNA signals from wild-type (x axis) and *pab2Δ* (y axis) cells. Red and green dots represent genes that demonstrated statistically significant upregulation and downregulation, respectively, in *pab2Δ* cells as determined by significance analysis of microarray (SAM).

(B) Upregulated snoRNAs as determined by expression profiling of *pab2Δ* cells. Asterisks indicate those snoRNAs identified by SAM (see Experimental Procedures for details).

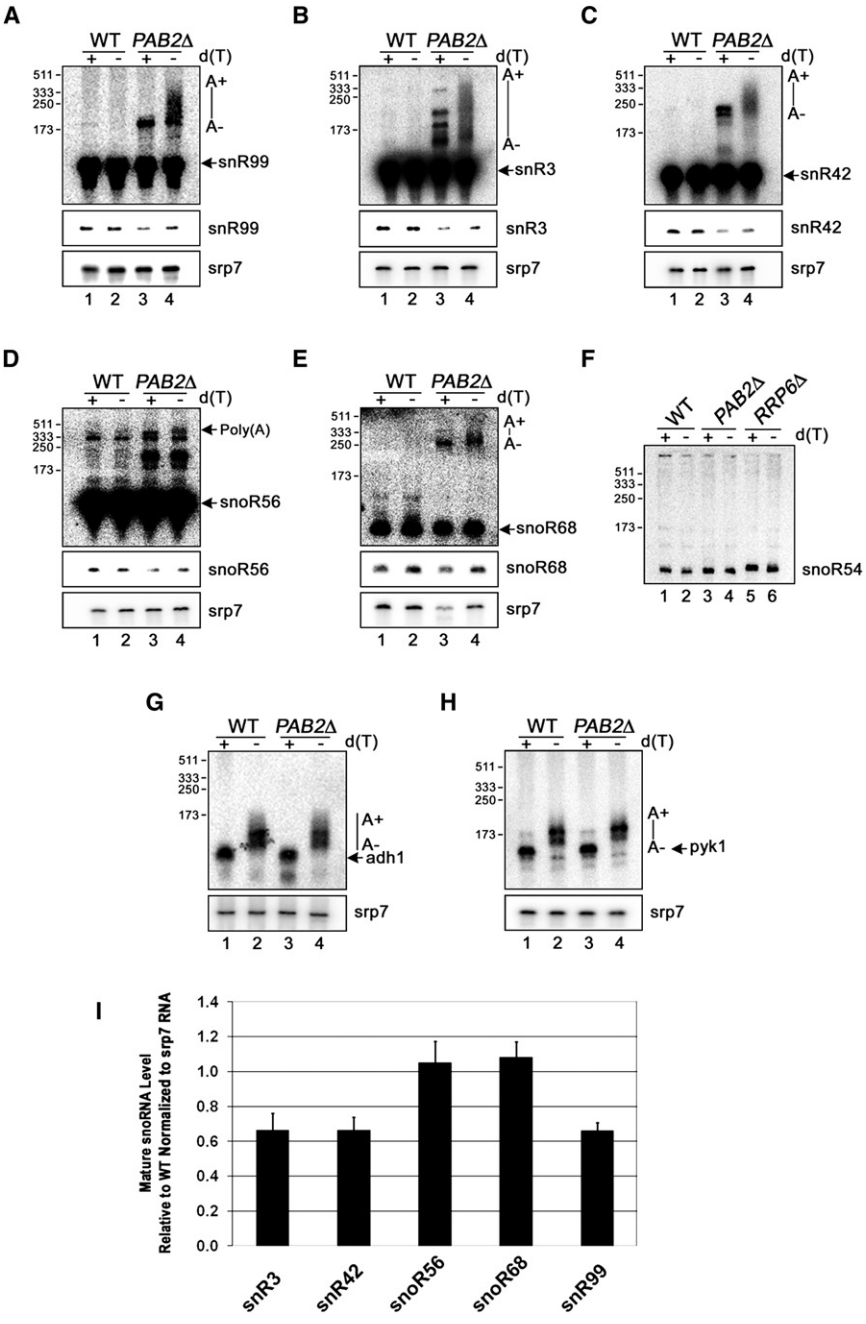

Figure 2. Accumulation of 3′-Extended Polyadenylated snoRNAs in *pab2Δ* Cells

(A–H) Total RNA prepared from wild-type and *pab2Δ* cells was treated with RNase H in the presence of DNA oligonucleotides complementary to H/ACA class snoRNAs snR99 (A), snR3 (B), and snR42 (C); C/D class snoRNAs snoR56 (D) and snoR68 (E); intron-derived snoR54 (F); and *adh1* (G) and *pyk1* (H) mRNAs. RNase H reactions were performed in the presence (+) or absence (−) of oligo(dT). srp7 RNA was used as a loading control. Size markers (in nucleotides) are indicated on the left.

(I) Quantification of alterations in mature snoRNA levels, with the wild-type ratio set to 1. Values represent the means of at least three independent experiments, and bars correspond to standard deviations.

and *pab2Δ* cells. Using a one-class comparison, we identified 113 and 85 genes that demonstrated increased and decreased RNA levels, respectively, in *pab2Δ* cells (Figure 1A and see Table S1 available online). Among these 198 misregulated RNAs are protein-coding genes that could be directly or indirectly regulated by Pab2. Interestingly, several noncoding small nucleolar RNAs (snoRNAs) also showed increased RNA levels in pab2Δ cells (Figure 1B). Because the role of PABPs in the control of nonconding RNA expression had not previously been described, we decided to address the mechanism by which snoRNAs were upregulated in the absence of Pab2.

pab2Δ Cells Accumulate 3′-Extended Polyadenylated snoRNAs

To independently validate the results obtained by DNA microarrays, we compared snoRNA levels between wild-type and *pab2Δ* strains by northern blotting. Surprisingly, larger heterogeneous populations of transcripts were specifically detected in the *pab2Δ* strain along with decreased levels of mature snoRNAs (data not shown). Given that we previously reported a hyperadenylation phenotype in *pab2Δ* cells (Perreault et al., 2007), we suspected that this heterogeneous RNA population could represent polyadenylated snoRNAs. To test this possibility, the 3′ end of several snoRNAs was examined by treating total RNA prepared from wild-type and *pab2Δ* cells with RNase H. RNase H treatment in the presence of a DNA oligonucleotide complementary to a region roughly 100 nt upstream from the mature 3′ end will release a 3′ fragment that can be detected by northern blot. As can be seen in Figure 2A, RNase H reactions using an oligo specific to H/ACA type snR99 yielded a 100 nt fragment corresponding to the 3′ end of mature snR99. Consistent with our northern blot assays, RNase H analyses from the *pab2Δ* strain showed heterogeneous 3′-extended snR99 products as well as decreased levels of mature snR99 (Figure 2A, lane 4, and Figure 2I). Importantly, addition of oligo d(T) to the RNase H reaction caused the heterogeneous population of 3′-extended snR99 transcripts to migrate as a discrete product (Figure 2A, lane 3). The collapse of heterogeneous 3′-extended snR99 transcripts into a discrete product after the addition of oligo d(T) suggests that 3′-extended snR99 are polyadenylated. This possibility was confirmed by

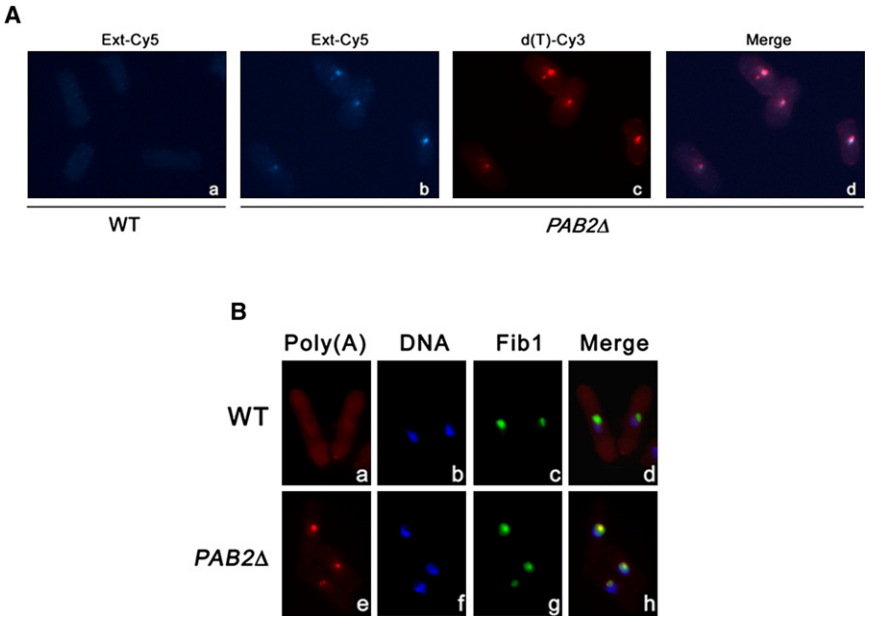

Figure 3. 3′-Extended snoRNAs Accumulate in Discrete Foci in *pab2Δ* Cells

(A) Wild-type (Aa) and *pab2Δ* cells (Ab–Ad) were analyzed by FISH after double labeling with a Cy5-labeled probe for 3′-extended snR99 (Aa and Ab) and a Cy3-labeled oligo(dT)$_{50}$ (Ac).

(B) Wild-type (Ba–Bd) and *pab2Δ* (Be–Bh) cells expressing GFP-tagged Fib1 were visualized for polyadenylated RNA using Cy3-labeled oligo(dT)$_{50}$ (Ba and Be), for DNA using DAPI (Bb and Bf), and for Fib1 using GFP (Bc and Bg).

sequencing 3′-extented snR99 transcripts after conversion to cDNA. DNA sequencing indicated the presence of nonencoded oligo(A) stretches 78 nt downstream from the mature 3′ end of snR99 (data not shown). A distance of 78 nt between the 3′ end of mature snR99 and the start of poly(A) tails is consistent with the detection of an ~178 nt product after RNase H cleavage using both d(T)$_{18}$ and snR99-specific oligos (Figure 2A, lane 3).

We next performed similar experiments to test whether polyadenylated products as seen for snR99 were observed for other snoRNAs in *pab2Δ* cells. Notably, all of the independently transcribed snoRNAs that were tested in *pab2Δ* cells accumulated oligo d(T)-sensitive 3′-extended heterogeneous products (Figures 2A–2E). The accumulation of polyadenylated snoRNAs in the *pab2Δ* strain was also associated with reduced levels of several mature snoRNAs (Figures 2A–2E and 2I). This analysis included two additional H/ACA box snoRNAs (snR3 and snR42; Figures 2B and 2C) as well as two C/D box snoRNAs that were not initially detected in the microarray experiments (snoR56 and snoR68; Figures 2D and 2E). In contrast to independently transcribed snoRNAs, 3′ end analysis of an intron-embedded C/D box snoRNA, snoR54, did not result in the accumulation of 3′-extended forms in *pab2Δ* cells (Figure 2F, lanes 3–4). As a control, a 3′-extended form of intron-embedded snoR54 accumulated in cells deleted for *rrp6* (Figure 2F, lanes 5–6), consistent with previous studies in budding yeast (Allmang et al., 1999a; van Hoof et al., 2000). We also analyzed the 3′ end of several mRNAs (Figures 2G and 2H and data not shown). As can be seen for the *adh1* and *pyk1* mRNAs, no differences in 3′ end decision and poly(A) tail length were detected between wild-type and *pab2Δ* cells. These experiments indicate that the absence of Pab2 leads to the accumulation of 3′-extended polyadenylated snoRNAs.

The accumulation of 3′-extended snoRNAs in *pab2Δ* cells could be the result of increased transcriptional readthrough as a consequence of defects in transcription termination. To address this possibility, we performed chromatin immunoprecipitation (ChIP) assays to examine the density of RNA Pol II along snoRNA genes. ChIP assays have previously been used in yeast to show 3′-extended Pol II crosslinking in mutants defective in transcription termination (Kim et al., 2006; Steinmetz et al., 2006; Thiebaut et al., 2006). Pol II densities as determined by ChIP were similar in regions 3′ of the H/ACA class *SNR99* gene between wild-type and *pab2Δ* strains (Figure S1). Comparable results were observed for two other snoRNA genes with polyadenylation sites 187 and 264 nt downstream from the mature snoRNA 3′ end (Figures S2 and S3). The ChIP assays suggest that the accumulation of 3′-extended snoRNAs in *pab2Δ* cells results from defects in a posttranscriptional mechanism, rather than the increased production of readthrough transcripts.

3′-Extented snoRNAs Accumulate in Discrete Foci in *pab2Δ* Cells

To determine the subcellular distribution of 3′-extended snoRNAs that accumulate in *pab2Δ* cells, a 54 nt probe was designed to specifically detect the 3′-extended form of H/ACA class snR99 by fluorescent in situ hybridization (FISH). Analysis of wild-type cells using this 54 nt probe produced background signal (Figure 3Aa), similar to control cells without the fluorescent probe (data not shown). This is consistent with the low level of 3′-extended snR99 detected in wild-type cells using RNase H assays (Figure 2A). In contrast, discrete foci were detected in *pab2Δ* cells using the fluorescent probe specific to 3′-extended snR99 (Figure 3Ab). Notably, these foci precisely coincided with poly(A)$^+$ RNA-rich foci (Figures 3Ab–3Ad) that are specifically detected in the absence of Pab2 (see below). This is consistent with the accumulation of 3′-extended polyadenylated snR99 in a discrete compartment of *pab2Δ* cells.

To further characterize the cellular localization of foci containing 3′-extended snR99 and poly(A)-rich RNA, oligo d(T) staining was combined with the DNA-intercalating agent DAPI that stains the nucleoplasm as well as with a GFP-tagged version of fibrillarin that localizes to the nucleolus. As can be seen in Figure 3B, poly(A)-rich foci were detected in *pab2Δ* cells (Figure 3Be), but not in wild-type cells (Figure 3Ba). Comparison of the different staining methods showed that the poly(A) bodies were concentrated in a region that was distinct from the DAPI staining but that colocalized with GFP signal (Figures 3Bf–3Bh). Such

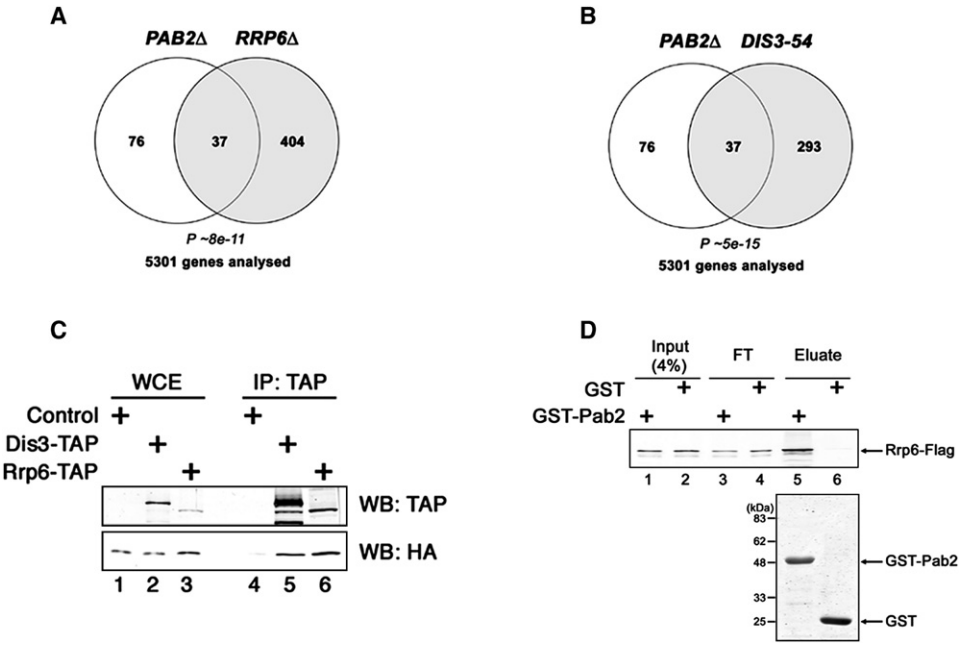

Figure 4. Functional and Physical Associations between Pab2 and the Nuclear Exosome

(A and B) Venn diagrams present the numbers of overlapping genes from the lists of genes that were upregulated ≥1.5-fold in the *pab2Δ* and *rrp6Δ* strains (A) and in the *pab2Δ* and *dis3-54* strains (B). The p values indicate the probabilities that the observed overlaps occurred by chance.

(C) Immunoblot analysis of whole-cell extracts (WCE; lanes 1–3) and IgG-Sepharose precipitates (IP; lanes 4–6) prepared from control, Dis3-TAP, and Rrp6-TAP cells expressing a HA-tagged version of Pab2.

(D) Direct interaction between Pab2 and Rrp6 in vitro. Equal amounts of purified Rrp6 were incubated with GST and GST-Pab2. Western blot (anti-Flag; upper panel) and corresponding Coomassie blue-stained loading control (lower panel) are shown. *FT*, flowthrough.

a specific colocalization between the poly(A) foci and Fib1-GFP was detected in the majority of *pab2Δ* cells. The results of the FISH experiments indicate that the nucleolus of *pab2Δ* cells accumulates polyadenylated RNAs, including 3′-extended forms of a snoRNA.

Functional and Physical Associations between Pab2 and the Nuclear Exosome

Given the similar levels in Pol II density downstream of snoRNA genes (Figures S1–S3), the accumulation of 3′-extended polyadenylated snoRNAs in the *pab2Δ* strain suggested that Pab2 functions via a posttranscriptional mechanism. To get insights into the pathway associated with Pab2-dependent snoRNA synthesis, we compared the expression profile of *pab2Δ* cells with the RNA profiles from all available fission yeast mutants to verify for significant overlap in regulated genes. Significantly, of those 113 Pab2-upregulated genes, 37 (33%) showed increased expression in cells deleted for the 3′→5′ exonuclease *rrp6* (Wilhelm et al., 2008) ($P \sim 8 \times 10^{-11}$), and similarly, 37 genes (33%) showed increased expression in the *dis3-54* strain (Wang et al., 2008) ($P \sim 5 \times 10^{-15}$) (Figures 4A and 4B). The *dis3-54* strain contains an amino acid substitution in the exonuclease domain of the exosome component Dis3/Rrp44 that impairs its catalytic activity (Murakami et al., 2007). Overall, 24 genes showed overlap between the lists of upregulated genes from *pab2Δ*, *rrp6Δ*, and *dis3-54* (Figure S4). These results underscore the important functional relationship among Pab2, Rrp6, and Dis3.

The significant overlap between the expression profiles of *pab2Δ*, *rrp6Δ*, and the *dis3-54* mutants suggested that Pab2 might physically interact with components of the exosome complex. To test this possibility, we affinity purified TAP-tagged versions of Rrp6 and Dis3 from extracts of cells that also expressed a HA-tagged version of Pab2. As can be seen in Figure 4C, Pab2 was coimmunoprecipitated with Dis3-TAP (lane 5) as well as with Rrp6-TAP (lane 6) but was not detected in a control purification (lane 4). These protein associations were not sensitive to RNases (data not shown). These results indicate that Rrp6 and Dis3 can be found in a complex with Pab2.

The results of the affinity purification experiments indicated that the enrichment of Pab2 in the Rrp6 purification was 16-fold greater than with Dis3 (Figure 4C). We therefore examined whether Pab2 makes direct contact with Rrp6. For this, the two proteins were expressed in *E. coli*, and the ability of purified Rrp6 to interact with GST-Pab2 was analyzed in vitro. Figure 4D shows that Rrp6 effectively bound to GST-Pab2 (lane 5), but not GST alone (lane 6). Similar results were obtained using soluble Pab2 and Rrp6 immobilized on beads (Figure S5). These experiments indicate that Pab2 directly interacts with Rrp6.

Pab2 Is Required for Rrp6-Dependent Processing but Functions in a Pathway Distinct from the Core Exosome

To further characterize the functional relationship between Pab2, Rrp6, and the core exosome, double mutants were generated. Deletion of *pab2* from a strain that expressed a catalytically

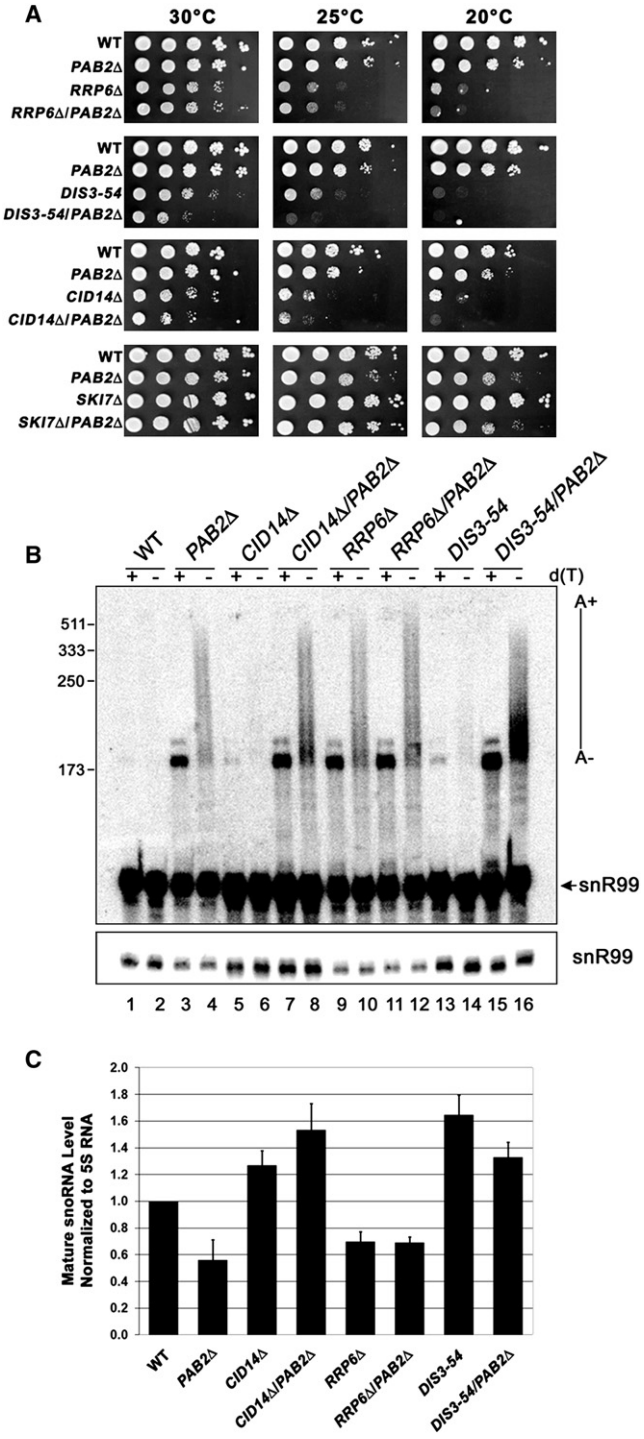

Figure 5. Pab2 Is Required for Rrp6-Dependent Processing but Functions in a Pathway Distinct from the Core Exosome

(A) Synthetic growth defects of *pab2Δ dis3-54* and *pab2Δ cid14Δ* double mutants.

(B) Equal amounts of total RNA prepared from the indicated strains were treated with RNase H in the presence of a DNA oligonucleotide complementary to H/ACA class snR99. RNase H reactions were performed in the presence (+) or absence (–) of oligo(dT). Size markers (in nucleotides) are indicated on the left.

(C) Quantification of alterations in mature snR99 levels, with the wild-type ratio set to 1. Values represent the means of at least three independent experiments, and bars correspond to standard deviations.

impaired version of Dis3 (*dis3-54*) exacerbated the growth defect of the *dis3-54* single mutant strain at all tested temperatures (Figure 5A). In contrast, the *pab2Δ rrp6Δ* double mutant strain showed a comparable growth rate to that of the *rrp6Δ* single mutant. These results suggest that whereas Pab2 and Rrp6 function in the same pathway, Pab2 and Dis3 function in distinct pathways. This conclusion was supported by RNA analyses, which demonstrated that the level of 3′-extended polyadenylated forms of snoRNA snR99, as well as the reduction in mature snR99 in the *pab2Δ rrp6Δ* double mutant, was similar to either single mutant strains (Figure 5B, compare lanes 11 and 12 to lanes 9 and 10 and 3 and 4; Figure 5C). Conversely, the level of 3′-extended poly(A)$^+$ forms of snR99 in the *pab2Δ dis3-54* double mutant was markedly increased relative to either single mutant strains (compare lanes 15 and 16 to 13 and 14 and 3 and 4); this was particularly noticeable for 3′-extended species of snR99 with short poly(A) tails. Furthermore, combining the *dis3-54* allele with the deletion of *pab2* restored the reduction of mature snoRNA detected in the *pab2Δ* single mutant (Figure 5B and 5C).

We also tested whether the polyadenylation of 3′-extended snoRNAs that accumulate in *pab2Δ* cells was dependent on the poly(A) polymerase activity of the TRAMP complex. We therefore deleted *cid14*, which encodes the single catalytic subunit of the fission yeast TRAMP complex (Win et al., 2006). As can be seen in Figure 5B, the length of poly(A) tails of 3′-extended snR99 in a *pab2Δ cid14Δ* double mutant strain was comparable to that of the single *pab2Δ* strain (compare lanes 7 and 8 to 3 and 4). Consistently, the poly(A) bodies that specifically accumulated in the nucleus of *pab2Δ* cells were still detected in the *pab2Δ cid14Δ* strain (Figure S6). These results suggest that Pab2 functions independently of the poly(A) polymerase activity of the TRAMP complex. Interestingly, the *pab2Δ cid14Δ* double mutant strain exhibited synthetic growth defects (Figure 5A). Moreover, deletion of *cid14* in the *pab2Δ* strain restored the lower levels of mature snoRNA seen in the *pab2Δ* single mutant (Figure 5A, compare lanes 7 and 8 to 3 and 4; Figure 5C), similar to the *pab2Δ dis3-54* double mutant.

Consistent with a nuclear-specific role for Pab2 in exosome-mediated snoRNA processing, cells deleted for *ski7*, which encodes a cytoplasmic-specific exosome-associated protein, did not accumulate 3′-extended polyadenylated snoRNA (Figure S7). Moreover, *ski7* demonstrated no genetic interaction with *pab2* (Figure 5A).

Taken together, these data suggest that Pab2 is required for Rrp6-dependent processing of 3′-extended polyadenylated snoRNAs. Conversely, although our results support a role for Dis3 and Cid14 in snoRNA metabolism, they appear to function in a pathway that diverges from that of Pab2.

Pab2 Is Recruited to the 3′ End of snoRNA Genes and Associates with Polyadenylated snoRNAs

mRNA 3′ end-processing events are tightly integrated to the transcription cycle through the carboxy-terminal domain of

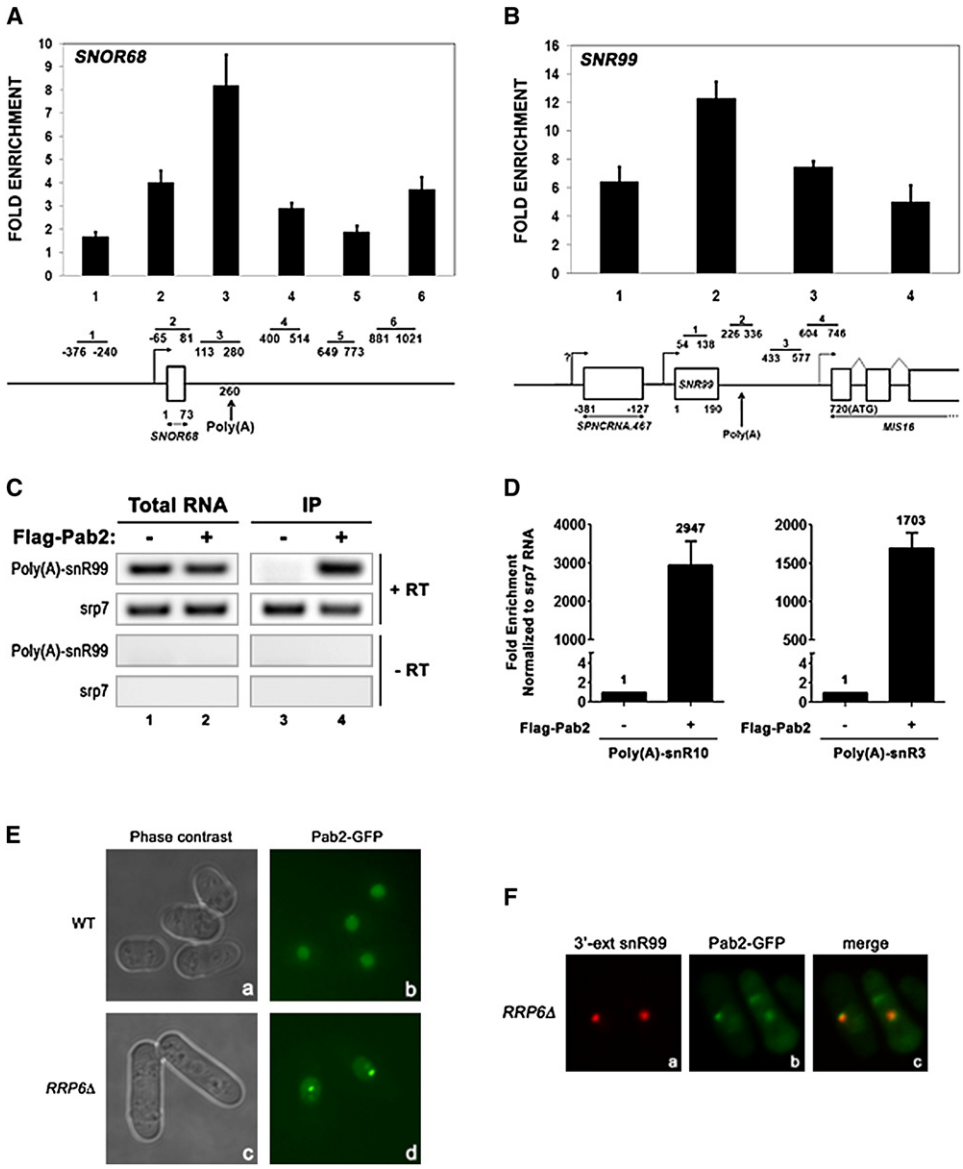

Figure 6. Recruitment of Pab2 to the 3′ End of snoRNA Genes

(A and B) ChIP assays were performed using a TAP-tagged version of Pab2. Coprecipitating DNA was quantified by real-time PCR using gene-specific primer pairs located along the (A) *SNOR68* and (B) *SNR99* genes. ChIP data are presented as the fold enrichment of Pab2 relative to a control region. Values represent the means of at least three independent experiments, and bars correspond to standard deviations. The position of the polyadenylation sites are indicated (poly[A]).

(C) RNA-IP experiments showing that polyadenylated snR99, but not the cytoplasmic srp7 RNA, is enriched in Flag-Pab2 precipitates. cDNA synthesis for snR99 and srp7 were oligo d(T) and random primed, respectively.

(D) Polyadenylated snoRNA association (IP:IN ratio) is normalized to srp7 RNA. Values were then set to 1.0 for the control immunoprecipitations. Values represent the means of at least two independent experiments, and bars correspond to standard deviations.

(E) Wild-type (Ea and Eb) and *rrp6Δ* cells (Ec and Ed) expressing a GFP-tagged version of Pab2 were visualized by phase contrast and for Pab2-GFP by live microscopy.

(F) *rrp6Δ* cells that expressed GFP-Pab2 were fixed and visualized by FISH using a probe for 3′-extended snR99 (Fa) as well as for GFP fluorescence (Fb).

RNA polymerase II (Buratowski, 2005; Hirose and Manley, 2000; Proudfoot, 2004). Accordingly, many factors involved in 3′ end processing/polyadenylation of mRNAs are recruited late during the transcription cycle and near the polyadenylation site of genes (Ahn et al., 2004; Kim et al., 2004). To determine whether Pab2 is associated with sites of snoRNA transcription, ChIP assays were performed using a TAP-tagged version of Pab2 (Lemieux and Bachand, 2009). Two independently transcribed snoRNA genes were monitored for Pab2 occupancy by ChIP: the C/D class *SNOR68* and the H/ACA class *SNR99*. Pab2 was strongly recruited to both *SNOR68* (Figure 6A) and *SNR99* (Figure 6B) genes. Significantly, Pab2 showed the greatest crosslinking

signal near the polyadenylation site of both snoRNA genes. These ChIP experiments indicate that Pab2 is recruited to sites of snoRNA transcription and that Pab2 is enriched near the polyadenylation site of two independent snoRNA genes.

We next examined whether Pab2 is bound to 3′-extended polyadenylated snoRNAs by RNA immunoprecipitation (RNA-IP) assays. Because 3′-extended polyadenylated snoRNAs are hardly detectable in wild-type cells (Figure 2), we performed these experiments in an *rrp6Δ* genetic background as these RNA species accumulate in the absence of Rrp6 (Figure 5). As can be seen in Figure 6C, a large enrichment of polyadenylated snR99 was observed in a Pab2 precipitate as compared to a control purification (upper panel, lanes 3 and 4). In contrast, the abundant cytoplasmic srp7 RNA was not enriched in precipitates of Pab2 (middle panel, lanes 3 and 4). No signal was detected in the absence of reverse transcription, indicating that the observed amplification was not due to the presence of residual DNA in the immunoprecipitates (Figure 6C, lower panels). Real-time RT-PCR analysis using primer sets to different snoRNAs confirmed the specific enrichment for other polyadenylated snoRNAs in Pab2 precipitates (Figure 6D). These results show that Pab2 is associated with polyadenylated snoRNAs.

We also examined whether the accumulation of 3′-extended snoRNAs perturbed the subcellular localization of Pab2. We therefore visualized the localization of a GFP-tagged version of Pab2 in wild-type and *rrp6Δ* cells. Whereas Pab2-containing foci were rarely observed in normal cells (Figure 6Eb), the absence of Rrp6 caused the concentration of Pab2 in specific nuclear foci (Figure 6Ed). Notably, the Pab2 foci in *rrp6Δ* cells coincided with foci corresponding to 3′-extended forms of snR99 (Figures 6Fa–6Fc). Taken together, these results suggest that poly(A)-bound Pab2 is found at sites of polyadenylated snoRNA accumulation.

DISCUSSION

PAPBs play essential roles in eukaryotic gene expression. Whereas PABPs play key functions in gene expression via the control of mRNAs, the role of PABPs in the expression of noncoding RNAs has never been reported. In the course of studying the function of the fission yeast PABPN1 homolog Pab2, we have performed a genome-wide study to address the functional significance of the nuclear PABP. In addition to identifying a novel function for the nuclear PABP in the synthesis of noncoding RNAs, our results provide important insights into exosome recruitment to polyadenylated RNA substrates.

Gene-Specific Regulation by Pab2 in Fission Yeast

Previous studies about PABPN1, which were based mainly on approaches using purified proteins and in vitro polyadenylation assays, have led to a model in which PABPN1 is critical for mRNA polyadenylation (Bienroth et al., 1993; Kerwitz et al., 2003; Wahle, 1991). It was surprising, therefore, given the important role of the 3′ poly(A) tail in mRNA expression, that the abundance of most transcripts was unaffected by the deletion of fission yeast *pab2*, as revealed by our microarray experiments. Furthermore, 3′ end analysis of several mRNAs by RNase H mapping between wild-type and *pab2Δ* strains showed no alteration in 3′ end decision and poly(A) tail length (Figure 2 and data not shown). Our findings argue that Pab2 is not a general factor required for mRNA polyadenylation, and therefore suggest that the regulation of mRNA poly(A) tail synthesis in the nucleus is likely to be more complex than previously anticipated.

The genome-wide approach used in this study indicated that several snoRNAs were upregulated in the absence of Pab2. Although the microarray results identified mostly H/ACA box snoRNAs (Figure 1), we showed that the absence of Pab2 results in the accumulation of 3′-extended polyadenylated forms of both C/D and H/ACA class snoRNAs (Figure 2). This bias toward the detection of H/ACA class snoRNAs in the microarray experiments is likely due to the generally larger size of H/ACA versus C/D box snoRNAs, which improves stable hybridization during microarray experiments. In addition, since RNase H assays detected 3′-extended polyadenylated forms of snoRNAs for which snoRNA probes did not produce usable signals on DNA microarrays, we believe that the number of snoRNAs that were affected by Pab2 was underestimated in our study. Given that poly(A) tails in *S. pombe* are on average 40 nt (Lackner et al., 2007), the accumulation of snoRNAs with poly(A) tails up to 300 nt in the absence of Pab2 (Figures 2 and 5) explains, at least in part, the hyperadenylation phenotype of *pab2Δ* cells (Perreault et al., 2007).

A Function for Pab2 in the Synthesis of Noncoding RNAs

Given the established role of PABPs in mRNA expression, the accumulation of polyadenylated forms of noncoding snoRNAs in *pab2Δ* cells was surprising. In the past few years, however, it has been established that polyadenylation not only provides stability to RNA molecules but also contributes to RNA processing via the exosome complex of 3′→5′ exonucleases. Accordingly, our study identified the nuclear exosome as the machinery that functions with Pab2 to promote processing of polyadenylated snoRNAs. The direct role of Pab2 in exosome-mediated processing of polyadenylated snoRNAs is supported by several observations: (1) Pab2 is physically associated with Rrp6 and Dis3 in vivo (Figure 4C), two exonucleases specific to the exosome; (2) Pab2 interacts directly with Rrp6 (Figure 4D); (3) microarray data indicate that the absence of Pab2 does not affect the expression of *rrp6* or any of the genes encoding for components of the core exosome (Figure 1A and data not shown); (4) Pab2 is recruited to the polyadenylation site of snoRNA genes (Figure 6); and (5) Pab2 is bound to 3′-extended polyadenylated snoRNAs (Figure 6). The role of the exosome in the processing of polyadenylated snoRNAs is therefore conserved between fission and budding yeasts as polyadenylated snoRNAs also accumulate in strains of *S. cerevisiae* lacking Rrp6 (Grzechnik and Kufel, 2008; van Hoof et al., 2000; Wyers et al., 2005). Our study therefore provides significant insights into exosome-dependent processing of polyadenylated snoRNAs by demonstrating the key role of a PABP in this process. Interestingly, the genome of *S. cerevisiae* does not encode for a homolog of fission yeast Pab2 and mammalian PABPN1 (Winstall et al., 2000), suggesting that a yet-to-be-identified PABP is likely involved in exosome-mediated processing of polyadenylated snoRNAs in budding yeast.

Our results also indicated that polyadenylation of the 3′-extended form of a snoRNA accumulating in the *pab2Δ*

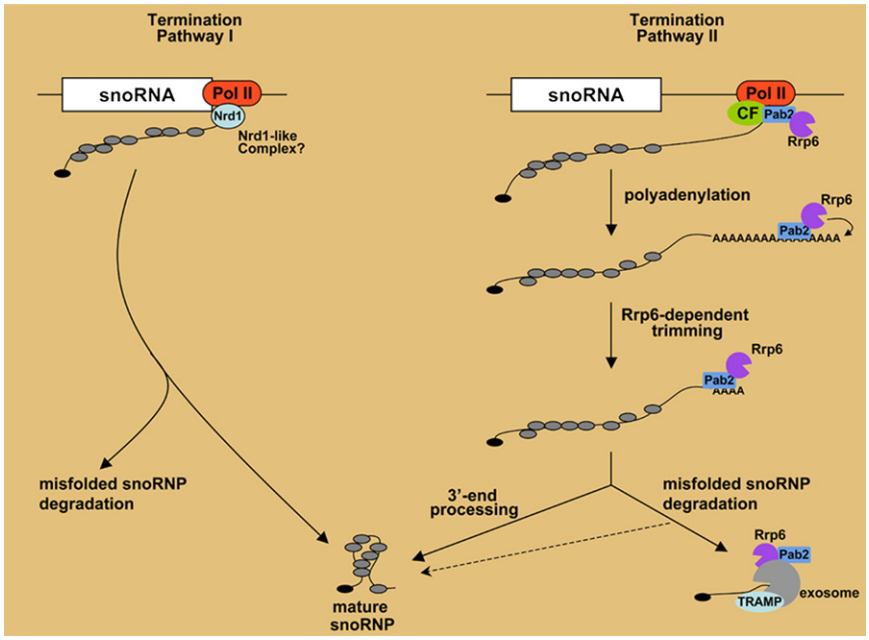

Figure 7. Model for the Role of Pab2 in snoRNA Synthesis

snoRNP proteins are cotranscriptionally recruited to nascent snoRNAs to control the biogenesis of snoRNPs. Two independent pathways function in snoRNA synthesis. The first generates mature snoRNPs via a system related to the budding yeast Nrd1/Nab3 complex using termination pathway I. Transcription complexes that escape the first termination system encounter a fail-safe termination pathway that uses an mRNA-like cleavage and polyadenylation complex (CF) to release 3′-extended pre-snoRNAs. Polyadenylation of pre-snoRNAs by the canonical poly(A) polymerase leads to the transfer of a Pab2/Rrp6 complex to the growing poly(A) tail and efficient 3′ end processing by Rrp6. Properly assembled snoRNPs will be shielded against complete exonucleolytic digestion by Rrp6. Defective snoRNAs that are not assembled into proper particles are directed to degradation by the nuclear exosome but can produce mature snoRNAs if pre-snoRNPs are allowed sufficient time for remodeling into proper particles.

mutant was independent of the poly(A) polymerase activity of the TRAMP complex. Given that we identified the canonical nuclear poly(A) polymerase, the product of the *S. pombe pla1* gene (homolog of *S. cerevisiae pap1*), as a Pab2-associated protein by tandem affinity purification (Lemieux and Bachand, 2009), we propose that Pla1 is responsible for the polyadenylation of 3′-extended snoRNA that accumulate in *pab2Δ* cells. Consistently, Pap1-dependent polyadenylation of snoRNAs has been reported (Carneiro et al., 2007; Grzechnik and Kufel, 2008; van Hoof et al., 2000; Wyers et al., 2005).

Despite the functional overlap between Rrp6 and Dis3, several studies using budding yeast demonstrate that depletion of these two nucleases can result in different RNA-processing defects (Allmang et al., 1999a; Dziembowski et al., 2007; Mitchell et al., 2003; van Hoof et al., 2000), suggesting that Rrp6 and Dis3 are responsible for distinctive steps in RNA processing. Furthermore, recent results now show that Rrp6 can perform specific processing events independently of the core exosome (Callahan and Butler, 2008). Our data using fission yeast are consistent with these aforementioned observations: although our genomic data indicated that Dis3, Rrp6, and Pab2 are functionally related (Figure 4 and Figure S4), the RNA-processing defects detected in the *rrp6Δ* and *dis3-54* strains were clearly distinct (Figure 5). Notably, the defects in snoRNA processing in the *pab2Δ* strain were most similar to those detected in *rrp6Δ* and *pab2Δ rrp6Δ* double mutants (Figure 5). In contrast, the absence of Pab2 expression in the context of a catalytically impaired core exosome (*dis3-54* allele) resulted in levels of polyadenylated snoRNAs greater than the *pab2Δ* and *dis3-54* single mutants. These results suggest that whereas Pab2 and Rrp6 function in the same pathway, Pab2 and the core exosome participate in overlapping but distinct pathways associated to snoRNA metabolism. This conclusion is consistent with the greater enrichment of Pab2 in the Rrp6 purification relative to the Dis3 purification (Figure 4C) and the direct interaction between Pab2 and Rrp6 (Figure 4D).

How does Pab2 function in snoRNA synthesis? Although a polyadenylation-independent pathway had previously been proposed to mediate 3′ end formation of snoRNAs in *S. cerevisiae* (Carroll et al., 2004; Fatica et al., 2000; Kim et al., 2006; Steinmetz et al., 2001; Vasiljeva and Buratowski, 2006), recent findings suggest that polyadenylation is involved in 3′ end maturation of snoRNA precursors by the exosome (Grzechnik and Kufel, 2008). Accordingly, the accumulation of 3′-extended polyadenylated snoRNAs together with the concurrent reduction of mature snoRNAs in the *pab2Δ*, *rrp6Δ*, and *pab2Δ rrp6Δ* double mutant strains (Figures 2 and 5) is consistent with a precursor-product relationship. Our ability to copurify polyadenylated snoRNAs with a snoRNP protein (Figure S8) is also consistent with the polyadenylated species being precursors to mature snoRNAs. These results support a model (Figure 7) in which 3′-extended polyadenylated snoRNAs that accumulate in *pab2Δ* cells correspond to pre-snoRNAs stalled or delayed in 3′ end processing, but that mature snoRNAs can still be synthesized via an independent pathway. This independent pathway could involve a fission yeast complex analogous to the Nrd1-Nab3-Sen1 complex that is involved in snoRNA termination and synthesis in budding yeast (Carroll et al., 2004; Kim et al., 2006; Steinmetz et al., 2001; Vasiljeva and Buratowski, 2006). Transcription complexes that escape the first termination pathway reach alternative termination sites that are recognized by an mRNA-like cleavage and polyadenylation machinery (Dheur et al., 2003; Garas et al., 2008). Polyadenylation of released 3′-extended snoRNAs provides high-affinity binding sites for Pab2 and favors the rapid transfer of Pab2 to the growing poly(A) tail. The exonucleolytic activity of Rrp6 carries out the processing of 3′-extended polyadenylated snoRNAs until it reaches a stable snoRNP complex, thus generating the mature snoRNA 3′ end.

Alternatively, defective snoRNP particles are recognized by exosome/TRAMP and directed to the degradation pathway. Defective particles can nevertheless return to the processing pathway if allowed sufficient time to remodel into stable snoRNPs, as suggested by our results in which the reduced levels of mature snoRNAs seen in *pab2Δ* cells were restored in the *pab2Δ dis3-54* and *pab2Δ cid14Δ* double mutant strains (Figure 5). Our model in which Pab2 promotes Rrp6 recruitment to poly(A) tails is interesting in light of the fact that recombinant Rrp6 is relatively inefficient at degrading a poly(A) substrate in vitro (Liu et al., 2006). Together, the aforementioned activities proposed for Pab2 significantly contribute to the efficient processing of polyadenylated snoRNAs since these RNA species are hardly detectable in normal cells.

Our study also provides interesting insights into the subcellular localization where processing of polyadenylated snoRNAs takes place. We found that a 3′-extended polyadenylated snoRNA localized to discrete nucleolar foci in *pab2Δ* and *rrp6Δ* cells. This echoes a report that polyadenylated snoRNAs accumulate in a specific nucleolar domain in *rrp6Δ* mutant of budding yeast (Carneiro et al., 2007). We further showed that Pab2 and a 3′-extended snoRNA were colocalized in similar foci in the *rrp6Δ* strain, suggesting that these foci represent processing centers where maturation of polyadenylated snoRNAs is delayed due to the absence of Rrp6. We envisage that misassembled snoRNPs that are directed to the exosome/TRAMP discard pathway are also degraded in these foci.

Conclusions

Our findings unveiled a function for a PABP in the expression of noncoding RNAs. Given the extensive similarity between the yeast and human nuclear PABPs, it is likely that the function of Pab2 in exosome-dependent RNA processing described here is evolutionarily conserved. The detection of poly(A) RNA-containing aggregates in the nucleus of muscle cells of individuals with mutations in *PABPN1* is a pathophysiological hallmark of the neuromuscular disorder, oculopharyngeal muscular dystrophy (OPMD). The intense accumulation of polyadenylated RNAs in a specific region of the nucleus brought about by the absence of *S. pombe* Pab2 is striking and raises the possibility that the intranuclear aggregates in OPMD are related to defects in the processing of noncoding RNAs.

EXPERIMENTAL PROCEDURES

DNA Microarray Analysis

cDNA synthesis of total RNAs, labeling, and microarray hybridization procedures have been described previously (Bachand et al., 2006). We determined statistical significance using significance analysis of microarray (SAM) (Tusher et al., 2001). Briefly, SAM provides a statistical value calculated for each gene based on the change in gene expression relative to the standard deviation of repeated measurements. The false discovery rate was set to be below 5%.

RNase H Analysis

Total yeast RNA was RNase H treated in a mixture containing message-specific oligonucleotides plus or minus oligo(dT) as previously described (Decker and Parker, 1993). RNA samples were resolved on 6% polyacrylamide-8 M urea gel, transferred onto nylon membranes, and probed using ^{32}P-labeled gene-specific probes.

Fluorescent In Situ Hybridization

3′-extended snR99 and poly(A)$^+$ RNA were visualized by FISH in *S. pombe* using a previously described method (Perreault et al., 2008). The 54-mer complementary to 3′-extended snR99 was conjugated with Cy5. The Cy5 signal in Figure 3A was converted to blue color using Adobe Photoshop to distinguish Cy5 and Cy3 signals. Control experiments using Cy5- and Cy3-labeled probes individually on *pab2Δ* cells confirmed the absence of bleed-through signal in the other channels (data not shown).

Expression of Recombinant Proteins and In Vitro Pull-Down Assays

GST and GST-Pab2 were expressed in *E. coli* and purified as described previously (Perreault et al., 2007). *S. pombe* Rrp6 was amplified by PCR using a fission yeast cDNA library (a generous gift from Charlie Hoffman) and expressed with a C-terminal Flag epitope in *E. coli*. For in vitro pull-down assays, equal amounts of Rrp6-coated beads were incubated with 1 μg of GST or GST-Pab2. The bound proteins were analyzed by immunoblotting using an Odyssey infrared imaging system.

RNA Immunoprecipitation Experiments

RNA IPs were performed as described previously (Ferreira-Cerca et al., 2007; Tardiff et al., 2006) using extracts prepared from a *pab2Δ rrp6Δ* double mutant strain that was previously transformed with a plasmid that express a Flag-tagged version of Pab2 or an empty control vector. Briefly, whole-cell extract was incubated with anti-Flag M2 beads. Following extensive washing steps, RNA was extracted from beads (IP RNA) and whole-cell extract (input RNA) using hot-phenol. RNA samples were treated with DNase I (Promega), and cDNA synthesis was primed with random hexamers (for srp7 RNA) and oligo d(T) (for polyadenylated snoRNAs). Quantitative real-time PCR was performed on a Realplex PCR machine (Eppendorf). Reported values are the averages of at least two independent experiments, and error bars represent ±1 SD.

Detailed methods are described in the Supplemental Information.

SUPPLEMENTAL INFORMATION

Supplemental Information includes one table, eight figures, Supplemental Experimental Procedures, and Supplemental References and can be found with this article online at doi:10.1016/j.molcel.2009.12.019.

ACKNOWLEDGMENTS

We thank R. Maraia, M. Yaganida, and P. Beauregard for strains and plasmids; P. Chartrand and F. Gallardo for advice on FISH microscopy; and S. Abou Elela and F. Dragon for critical reading of the manuscript. We also thank S. Khadayate for microarray data deposition. This work was funded by grants from the Natural Sciences and Engineering Research Council of Canada (NSERC) (to F.B.) and from Cancer Research UK (to J.B.). J.-F.L. was supported by a Scholarship from NSERC. F.B. is the recipient of a New Investigator Award from the Canadian Institutes of Health Research (CIHR) and a Career Development Award from the Human Frontier Science Program Organization (HFSPO).

Received: May 5, 2009
Revised: August 11, 2009
Accepted: November 9, 2009
Published: January 14, 2010

REFERENCES

Ahn, S.H., Kim, M., and Buratowski, S. (2004). Phosphorylation of serine 2 within the RNA polymerase II C-terminal domain couples transcription and 3′ end processing. Mol. Cell *13*, 67–76.

Allmang, C., Kufel, J., Chanfreau, G., Mitchell, P., Petfalski, E., and Tollervey, D. (1999a). Functions of the exosome in rRNA, snoRNA and snRNA synthesis. EMBO J. *18*, 5399–5410.

Allmang, C., Petfalski, E., Podtelejnikov, A., Mann, M., Tollervey, D., and Mitchell, P. (1999b). The yeast exosome and human PM-Scl are related complexes of 3′→5′ exonucleases. Genes Dev. *13*, 2148–2158.

Allmang, C., Mitchell, P., Petfalski, E., and Tollervey, D. (2000). Degradation of ribosomal RNA precursors by the exosome. Nucleic Acids Res. *28*, 1684–1691.

Arigo, J.T., Eyler, D.E., Carroll, K.L., and Corden, J.L. (2006). Termination of cryptic unstable transcripts is directed by yeast RNA-binding proteins Nrd1 and Nab3. Mol. Cell *23*, 841–851.

Bachand, F., Lackner, D.H., Bahler, J., and Silver, P.A. (2006). Autoregulation of ribosome biosynthesis by a translational response in fission yeast. Mol. Cell. Biol. *26*, 1731–1742.

Bienroth, S., Keller, W., and Wahle, E. (1993). Assembly of a processive messenger RNA polyadenylation complex. EMBO J. *12*, 585–594.

Bousquet-Antonelli, C., Presutti, C., and Tollervey, D. (2000). Identification of a regulated pathway for nuclear pre-mRNA turnover. Cell *102*, 765–775.

Buratowski, S. (2005). Connections between mRNA 3′ end processing and transcription termination. Curr. Opin. Cell Biol. *17*, 257–261.

Callahan, K.P., and Butler, J.S. (2008). Evidence for core exosome independent function of the nuclear exoribonuclease Rrp6p. Nucleic Acids Res. *36*, 6645–6655.

Carneiro, T., Carvalho, C., Braga, J., Rino, J., Milligan, L., Tollervey, D., and Carmo-Fonseca, M. (2007). Depletion of the yeast nuclear exosome subunit Rrp6 results in accumulation of polyadenylated RNAs in a discrete domain within the nucleolus. Mol. Cell. Biol. *27*, 4157–4165.

Carroll, K.L., Pradhan, D.A., Granek, J.A., Clarke, N.D., and Corden, J.L. (2004). Identification of cis elements directing termination of yeast nonpolyadenylated snoRNA transcripts. Mol. Cell. Biol. *24*, 6241–6252.

Chekanova, J.A., Gregory, B.D., Reverdatto, S.V., Chen, H., Kumar, R., Hooker, T., Yazaki, J., Li, P., Skiba, N., Peng, Q., et al. (2007). Genome-wide high-resolution mapping of exosome substrates reveals hidden features in the Arabidopsis transcriptome. Cell *131*, 1340–1353.

Decker, C.J., and Parker, R. (1993). A turnover pathway for both stable and unstable mRNAs in yeast: evidence for a requirement for deadenylation. Genes Dev. *7*, 1632–1643.

Dez, C., Houseley, J., and Tollervey, D. (2006). Surveillance of nuclear-restricted pre-ribosomes within a subnucleolar region of Saccharomyces cerevisiae. EMBO J. *25*, 1534–1546.

Dheur, S., Vo le, T.A., Voisinet-Hakil, F., Minet, M., Schmitter, J.M., Lacroute, F., Wyers, F., and Minvielle-Sebastia, L. (2003). Pti1p and Ref2p found in association with the mRNA 3′ end formation complex direct snoRNA maturation. EMBO J. *22*, 2831–2840.

Dziembowski, A., Lorentzen, E., Conti, E., and Seraphin, B. (2007). A single subunit, Dis3, is essentially responsible for yeast exosome core activity. Nat. Struct. Mol. Biol. *14*, 15–22.

Fatica, A., Morlando, M., and Bozzoni, I. (2000). Yeast snoRNA accumulation relies on a cleavage-dependent/polyadenylation-independent 3′-processing apparatus. EMBO J. *19*, 6218–6229.

Ferreira-Cerca, S., Poll, G., Kuhn, H., Neueder, A., Jakob, S., Tschochner, H., and Milkereit, P. (2007). Analysis of the in vivo assembly pathway of eukaryotic 40S ribosomal proteins. Mol. Cell *28*, 446–457.

Garas, M., Dichtl, B., and Keller, W. (2008). The role of the putative 3′ end processing endonuclease Ysh1p in mRNA and snoRNA synthesis. RNA *14*, 2671–2684.

Grzechnik, P., and Kufel, J. (2008). Polyadenylation linked to transcription termination directs the processing of snoRNA precursors in yeast. Mol. Cell *32*, 247–258.

Hirose, Y., and Manley, J.L. (2000). RNA polymerase II and the integration of nuclear events. Genes Dev. *14*, 1415–1429.

Houseley, J., and Tollervey, D. (2006). Yeast Trf5p is a nuclear poly(A) polymerase. EMBO Rep. *7*, 205–211.

Houseley, J., LaCava, J., and Tollervey, D. (2006). RNA-quality control by the exosome. Nat. Rev. Mol. Cell Biol. *7*, 529–539.

Ibrahim, H., Wilusz, J., and Wilusz, C.J. (2008). RNA recognition by 3′-to-5′ exonucleases: the substrate perspective. Biochim. Biophys. Acta *1779*, 256–265.

Kadaba, S., Wang, X., and Anderson, J.T. (2006). Nuclear RNA surveillance in Saccharomyces cerevisiae: Trf4p-dependent polyadenylation of nascent hypomethylated tRNA and an aberrant form of 5S rRNA. RNA *12*, 508–521.

Kerwitz, Y., Kuhn, U., Lilie, H., Knoth, A., Scheuermann, T., Friedrich, H., Schwarz, E., and Wahle, E. (2003). Stimulation of poly(A) polymerase through a direct interaction with the nuclear poly(A) binding protein allosterically regulated by RNA. EMBO J. *22*, 3705–3714.

Kim, M., Ahn, S.H., Krogan, N.J., Greenblatt, J.F., and Buratowski, S. (2004). Transitions in RNA polymerase II elongation complexes at the 3′ ends of genes. EMBO J. *23*, 354–364.

Kim, M., Vasiljeva, L., Rando, O.J., Zhelkovsky, A., Moore, C., and Buratowski, S. (2006). Distinct pathways for snoRNA and mRNA termination. Mol. Cell *24*, 723–734.

Kiss, T., Fayet, E., Jady, B.E., Richard, P., and Weber, M. (2006). Biogenesis and intranuclear trafficking of human box C/D and H/ACA RNPs. Cold Spring Harb. Symp. Quant. Biol. *71*, 407–417.

Kuhn, U., and Wahle, E. (2004). Structure and function of poly(A) binding proteins. Biochim. Biophys. Acta *1678*, 67–84.

LaCava, J., Houseley, J., Saveanu, C., Petfalski, E., Thompson, E., Jacquier, A., and Tollervey, D. (2005). RNA degradation by the exosome is promoted by a nuclear polyadenylation complex. Cell *121*, 713–724.

Lackner, D.H., Beilharz, T.H., Marguerat, S., Mata, J., Watt, S., Schubert, F., Preiss, T., and Bahler, J. (2007). A network of multiple regulatory layers shapes gene expression in fission yeast. Mol. Cell *26*, 145–155.

Lebreton, A., and Seraphin, B. (2008). Exosome-mediated quality control: substrate recruitment and molecular activity. Biochim. Biophys. Acta *1779*, 558–565.

Lemieux, C., and Bachand, F. (2009). Cotranscriptional recruitment of the nuclear poly(A)-binding protein Pab2 to nascent transcripts and association with translating mRNPs. Nucleic Acids Res. *37*, 3418–3430.

Liu, Q., Greimann, J.C., and Lima, C.D. (2006). Reconstitution, activities, and structure of the eukaryotic RNA exosome. Cell *127*, 1223–1237.

Mangus, D.A., Evans, M.C., and Jacobson, A. (2003). Poly(A)-binding proteins: multifunctional scaffolds for the post-transcriptional control of gene expression. Genome Biol. *4*, 223.

Milligan, L., Torchet, C., Allmang, C., Shipman, T., and Tollervey, D. (2005). A nuclear surveillance pathway for mRNAs with defective polyadenylation. Mol. Cell. Biol. *25*, 9996–10004.

Mitchell, P., Petfalski, E., Houalla, R., Podtelejnikov, A., Mann, M., and Tollervey, D. (2003). Rrp47p is an exosome-associated protein required for the 3′ processing of stable RNAs. Mol. Cell. Biol. *23*, 6982–6992.

Murakami, H., Goto, D.B., Toda, T., Chen, E.S., Grewal, S.I., Martienssen, R.A., and Yanagida, M. (2007). Ribonuclease activity of Dis3 is required for mitotic progression and provides a possible link between heterochromatin and kinetochore function. PLoS ONE *2*, e317. 10.1371/journal.pone.0000317.

Perreault, A., Lemieux, C., and Bachand, F. (2007). Regulation of the nuclear poly(A)-binding protein by arginine methylation in fission yeast. J. Biol. Chem. *282*, 7552–7562.

Perreault, A., Bellemer, C., and Bachand, F. (2008). Nuclear export competence of pre-40S subunits in fission yeast requires the ribosomal protein Rps2. Nucleic Acids Res. *36*, 6132–6142.

Proudfoot, N. (2004). New perspectives on connecting messenger RNA 3′ end formation to transcription. Curr. Opin. Cell Biol. *16*, 272–278.

Reichow, S.L., Hamma, T., Ferre-D'Amare, A.R., and Varani, G. (2007). The structure and function of small nucleolar ribonucleoproteins. Nucleic Acids Res. *35*, 1452–1464.

Saguez, C., Schmid, M., Olesen, J.R., Ghazy, M.A., Qu, X., Poulsen, M.B., Nasser, T., Moore, C., and Jensen, T.H. (2008). Nuclear mRNA surveillance

in THO/sub2 mutants is triggered by inefficient polyadenylation. Mol. Cell *31*, 91–103.

Schmid, M., and Jensen, T.H. (2008). The exosome: a multipurpose RNA-decay machine. Trends Biochem. Sci. *33*, 501–510.

Steinmetz, E.J., Conrad, N.K., Brow, D.A., and Corden, J.L. (2001). RNA-binding protein Nrd1 directs poly(A)-independent 3′-end formation of RNA polymerase II transcripts. Nature *413*, 327–331.

Steinmetz, E.J., Warren, C.L., Kuehner, J.N., Panbehi, B., Ansari, A.Z., and Brow, D.A. (2006). Genome-wide distribution of yeast RNA polymerase II and its control by Sen1 helicase. Mol. Cell *24*, 735–746.

Tardiff, D.F., Lacadie, S.A., and Rosbash, M. (2006). A genome-wide analysis indicates that yeast pre-mRNA splicing is predominantly posttranscriptional. Mol. Cell *24*, 917–929.

Thiebaut, M., Kisseleva-Romanova, E., Rougemaille, M., Boulay, J., and Libri, D. (2006). Transcription termination and nuclear degradation of cryptic unstable transcripts: a role for the nrd1-nab3 pathway in genome surveillance. Mol. Cell *23*, 853–864.

Tusher, V.G., Tibshirani, R., and Chu, G. (2001). Significance analysis of microarrays applied to the ionizing radiation response. Proc. Natl. Acad. Sci. USA *98*, 5116–5121.

Vanacova, S., and Stefl, R. (2007). The exosome and RNA quality control in the nucleus. EMBO Rep. *8*, 651–657.

Vanacova, S., Wolf, J., Martin, G., Blank, D., Dettwiler, S., Friedlein, A., Langen, H., Keith, G., and Keller, W. (2005). A new yeast poly(A) polymerase complex involved in RNA quality control. PLoS Biol. *3*, e189. 10.1371/journal.pbio.0030189.

van Hoof, A., Lennertz, P., and Parker, R. (2000). Yeast exosome mutants accumulate 3′-extended polyadenylated forms of U4 small nuclear RNA and small nucleolar RNAs. Mol. Cell. Biol. *20*, 441–452.

Vasiljeva, L., and Buratowski, S. (2006). Nrd1 interacts with the nuclear exosome for 3′ processing of RNA polymerase II transcripts. Mol. Cell *21*, 239–248.

Vasiljeva, L., Kim, M., Terzi, N., Soares, L.M., and Buratowski, S. (2008). Transcription termination and RNA degradation contribute to silencing of RNA polymerase II transcription within heterochromatin. Mol. Cell *29*, 313–323.

Wahle, E. (1991). A novel poly(A)-binding protein acts as a specificity factor in the second phase of messenger RNA polyadenylation. Cell *66*, 759–768.

Wahle, E. (1995). Poly(A) tail length control is caused by termination of processive synthesis. J. Biol. Chem. *270*, 2800–2808.

Wang, S.W., Stevenson, A.L., Kearsey, S.E., Watt, S., and Bahler, J. (2008). Global role for polyadenylation-assisted nuclear RNA degradation in posttranscriptional gene silencing. Mol. Cell. Biol. *28*, 656–665.

West, S., Gromak, N., Norbury, C.J., and Proudfoot, N.J. (2006). Adenylation and exosome-mediated degradation of cotranscriptionally cleaved pre-messenger RNA in human cells. Mol. Cell *21*, 437–443.

Wilhelm, B.T., Marguerat, S., Watt, S., Schubert, F., Wood, V., Goodhead, I., Penkett, C.J., Rogers, J., and Bahler, J. (2008). Dynamic repertoire of a eukaryotic transcriptome surveyed at single-nucleotide resolution. Nature *453*, 1239–1243.

Win, T.Z., Draper, S., Read, R.L., Pearce, J., Norbury, C.J., and Wang, S.W. (2006). Requirement of fission yeast Cid14 in polyadenylation of rRNAs. Mol. Cell. Biol. *26*, 1710–1721.

Winstall, E., Sadowski, M., Kuhn, U., Wahle, E., and Sachs, A.B. (2000). The Saccharomyces cerevisiae RNA-binding protein Rbp29 functions in cytoplasmic mRNA metabolism. J. Biol. Chem. *275*, 21817–21826.

Wyers, F., Rougemaille, M., Badis, G., Rousselle, J.C., Dufour, M.E., Boulay, J., Regnault, B., Devaux, F., Namane, A., Seraphin, B., et al. (2005). Cryptic pol II transcripts are degraded by a nuclear quality control pathway involving a new poly(A) polymerase. Cell *121*, 725–737.